Memoirs of the Faculty of Engineering, Kyushu University, Vol.65, No.2, June 2005

Experimental Study on Freezing Behavior of Molten Metal on Structure

by

M. Mizanur RAHMAN*, Tomohiko HINO*, Koji MORITA**, Tatsuya MATSUMOTO***,
Kiyoshi NAKAGAWA†, Kenji FUKUDA†† and Werner MASCHEK†††

(Received May 9, 2005)

Abstract

Freezing behavior of molten metal during interaction with core structure was studied with respect to safety of liquid metal reactor (LMR). In this study, wood's metal (melting point 78.8°C) was used as a simulant melt while stainless steel and copper were used as freezing structures. A series of simulation experiments was conducted to study the freezing behavior of wood's metal during pouring up on the freezing structures immersed into the coolant. In the experiment, simulant melt was poured in a stainless steel tube and finally injected into coolants through nozzle to obtain the freezing behavior of the molten metal. The penetration length and width were measured in air coolant experiment where as the penetration length and amount of adhered frozen metal were measured in water coolant experiment. The melt flow and distribution were observed for both the experiments with a high-speed video camera. The experiment shows that higher penetration length and good adherence on structure was found in air coolant experiment than the water coolant experiment. The data obtained in this experiment can also be used as a reference database while simulating with relevant computational codes.

Keywords: Liquid metal reactor (LMR), Reactor safety, Freezing phenomena, Molten metal, Penetration length

1. Introduction

The freezing of molten metal during interaction with core structure is one of the major concerns for the safety of the liquid metal (specially lead bismuth eutectic) cooled reactor that happens following hypothetical core disruptive accidents (CDAs).[1)] Interaction of molten fuel and structure can occur only when serious transient over power (TOP) and transient under cooling (TUC) accident take place,[2)] which are, often called CDAs. These include fuel pin disruption, transition or subassembly disruption and escape of fuel. This is because they potentially lead to significant mechanical energy release as a result of re-criticality or interaction of molten metal and structure during core meltdown process.

Hypothetical accidents in Liquid Metal Reactor (LMR) can lead to disassembly of the core, which influences the freezing process of molten metal on reactor subassembly structure. As the core disassembly expansion increases, molten fuel is ejected up into the above core subassembly

* Graduate Student, Department of Applied Quantum Physics and Nuclear Engineering
** Associate Professor, Institute of Environmental Systems
*** Research Associate, Institute of Environmental Systems
† Technical Assistant, Department of Applied Quantum Physics and Nuclear Engineering
†† Professor, Institute of Environmental Systems
††† Institute for Nuclear and Energy Technologies, Forschungszentrum Karlsruhe, Germany

structure. If this fuel can pass-up through and out of the top of the subassemblies, it can be largely discounted from further criticality considerations. If the fuel can freeze and plug in the above core structure, it can potentially re-melt due to decay heat and relocation in the core region and subsequently blockage the subassembly.[3] The safe containment of molten fuel in a LMR following a CDA depends strongly on the post accident distribution of such materials/post accident heat removal from these materials. It is crucial to understand re-embodiment of this type because it can produce secondary excursions. One important aspects of this problem is an assessment of freezing phenomena of molten metal in the subassembly structure during CDA for the viewpoint of LMR safety.[4]

Substantial attention has been drawn recently about the freezing of liquid metals in subassembly structure for safety analysis of reactor severe accidents.[6-10] The present paper deals with concerning the observation of freezing behavior with the viewpoint of the safety of LMR. The main objective of the present study is to understand the basic physical phenomena and determination of some characteristics parameters of freezing of molten metal during penetration into the core structure. This key phenomena of production of material distribution and penetration length of molten metal can be observed when supercooling liquid come close to the structure. Thus, in order to observe the freezing behavior of molten metal on core structure, a series of basic freezing experiments was performed varying the size of nozzles, properties of melt and structure. The result obtained in this experiment can be used as a database for the safety analysis of the LMR.

In the present study, freezing experiment is performed in order to get the freezing behavior of the molten metal that includes penetration length, width, amount of adhered frozen metal and penetration history of the molten metal during falling through the nozzle. In this experiment, Wood's metal with the composition of Bi 60%, Sn 20% and In 20% is used as a simulant molten metal since its density and thermal conductivity those are similar of the reactor core material. Its melting point is low (78.8^{o}C) and boiling point is high (1760^{o}C). Some physical properties of Wood's metal are given in **Table 1.**

Table 1 Some physical properties of Wood's metal.[1, 5]

Parameters	Value
Melting point	78.8^{o}C
Boiling Point	1760^{o}C
Density	8100 kg/m^{3}
Thermal conductivity	11.1 W/m.K
Specific heat	150 J/kg.K
Volume expansion coefficient	2.2×10^{-5}/K
Kinematic viscosity	2×10^{-5} m^{2}/s
Latent heat of fusion	2.53×10^{4} J/kg
Liquidus temperature	397 K
Surface tension	~1.0 N/m
Composition: Bi, Sn and In	60%, 20% and 20%

2. Outline of the Experiment

2.1 Experimental set-up

The present freezing experiment is conducted using two types of coolant such as air and water. The experimental facility consists of melt tank in which molten metal is poured. Nozzle is connected at the bottom of the melt tank to generate a smooth melt flow is ejected onto the metal structure. Melt tank and nozzle are heated by an electric heater adjusting their temperature by the temperature controller. Thirty one of k-type thermocouples are connected with the melt tank, nozzle and metal structure to measure the temperature of the melt during falling onto the metal structure.

The melt tank and nozzle are made of stainless steel. The inner diameter of the upper part of the melt tank is 75 mm where as the inner and outer diameter of the lower part of the melt tank is 12.5 and 37.5 mm, respectively. Three different nozzles of no. 1, 2 and 3 of sizes 50 mm × 0.5 mm, 50 mm × 0.8 mm and 50 mm × 1.0 mm, respectively, are used for the smooth ejection of melt onto the metal structure. The water tank, which is a rectangular type open-topped box of dimension 1500 mm × 300 mm, is made of stainless steel and two sides of walls are made of transparent glass for the

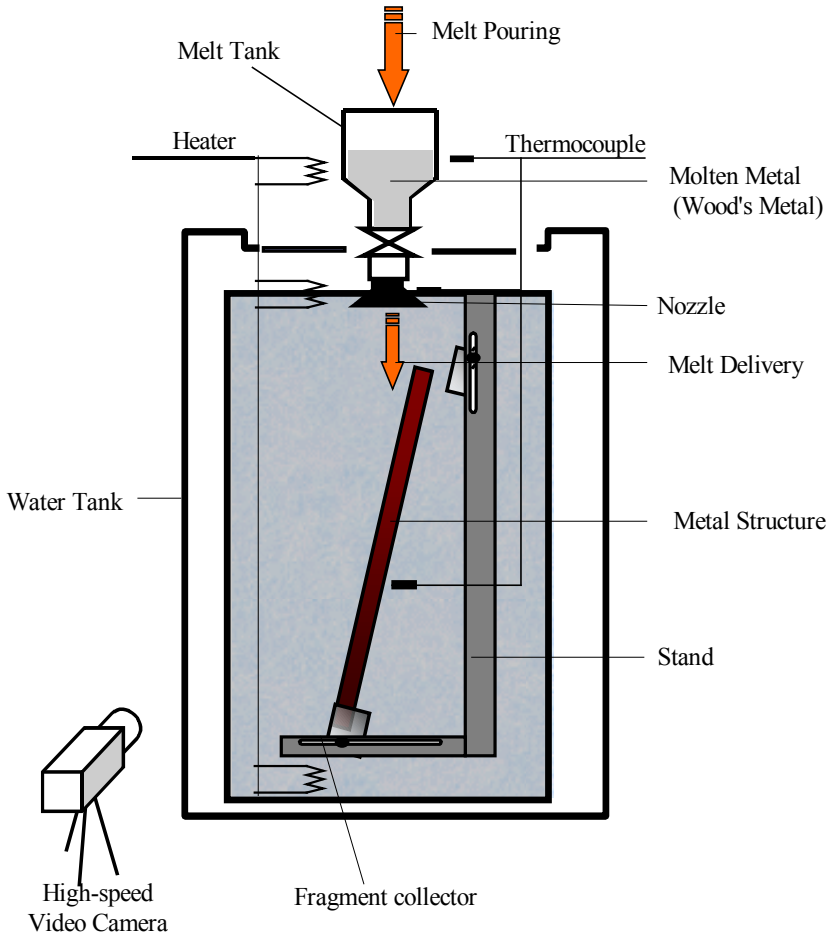

Fig. 1 Schematic of experimental set-up.

purpose of visualization. An electric heater with temperature controller and a thermocouple sensor are used to control the water temperature at a desired level. The metal structure is supported with a stainless steel stand with a fragment collector inside the stand. During air coolant experiment, only the water pool was absent. A high-speed video camera (SONY, Model: DCR-TRV900) was used to record the video images of the melt during falling onto the metal structure.

Using this facility, a series of freezing experiment is conducted by interacting molten metal with structure using air and water coolant to investigate experimentally the freezing phenomena of molten metal during core meltdown of LMRs under CDA. Out of a series of experiments, some good results have been selected and presented in this paper. The main objective of this experiment is to study the behavior of freezing of molten metal on core structure and to determine some physical parameters which includes the penetration length, width and amount of adhered frozen metal during freezing on core structure.

2.2 Experimental procedure

2.2.1 Air coolant experiment

The experiment is conducted in two steps using two types of coolant such as air and water. The freezing phenomena are investigated experimentally using two candidate structures such as Stainless Steel and Cooper. In air coolant experiment, simulant Wood's metal is heated by a gas burner, transferred to the test section, the temperature of the melt is monitored by digital thermometer and poured into the melt tank. In this tank, temperature is measured again to achieve the desired temperature. After reached at the desired temperature, the melt is injected onto the structure by opening the plug of the nozzle. The freezing behavior during interaction of molten metal and structures are observed in air coolant condition. A high-speed video camera is used for observation of freezing behavior. The experiments are performed by changing the structure, nozzle, temperature of the molten metal and volume of molten metal. The frozen layer and other fragments are collected after each experiment. The measuring parameters, such as penetration length is the length of the frozen metal adhered on structure and width is the average uniform width of the frozen metal adhered on structure are carried out by the conventional measuring tape and the melt flow rate is determined by measuring the falling time using stop watch and then divided the amount of frozen metal by falling time. The experimental conditions are summarized in **Table 2**.

Table 2 Air coolant experimental conditions.

Structure	copper	stainless steel	
Nozzle size (mm×mm)	50×0.50 (Nozzle no. 1)	50×0.80 (Nozzle no. 2)	50×1.0 (Nozzle no. 3)
Melt mass (g)	350	500	

2.2.2 Water coolant experiment

At first, the structure is set up in the water tank and after then the cylindrical stainless steel tank and the nozzle section are transferred to the top of the water tank and fixed it up. The temperature of the water tank is controlled at specific temperature by the electric heater. The molten metal is prepared as described in section 2.2.1 and poured into the cylindrical tank. In this tank, the temperature is measured to achieve the desired temperature. Molten metal at desired temperature is ejected into the structure by opening the plug of the nozzle. In this experiment, only nozzle no. 1 is used. The freezing behavior of molten metal on structures is investigated in water coolant condition. First, experiments are conducted by changing the water temperature for fixing up the water temperature. After fixing up the water temperature, experiments are performed by changing structure, the temperature and volume of the molten metal. The frozen layer and other fragments are collected after each experiment and the measurements are carried out as described in section 2.2.1. In both air and water coolant conditions, experiments are carried out at atmospheric pressure. The experimental conditions are summarized in **Table 3**.

Table 3 Water coolant experimental conditions.

Structure	copper	stainless steel
Nozzle size (mm×mm)	50×0.50	
Melt mass (g)	350	200

3. Experimental Results and Discussion

3.1 Visual observation and analysis

3.1.1 Air coolant experiment

In case of cooper structure, three nozzles of different sizes are used to get different flow rates. Wood's metal of 350 g is used as molten metal and the melt flow rate of nozzle no. 1, 2 and 3

were evaluated as 110, 240 and 270 g/s, respectively. In case of stainless steel structure, Wood's metal of 500 g and only nozzle no. 1 is used. The experiments were conducted by changing the melt temperature at the range of 89.8-110°C, 95-120°C and 88.5-98°C for nozzle no. 1, 2 and 3 respectively. The typical freezing behaviors of molten metal are shown in **Figs. 2 and 3**. The pictures on the left side show the freezing behavior of molten metal on copper structure while on the right shows the freezing behavior of same molten metal on stainless steel structure during falling in the air.

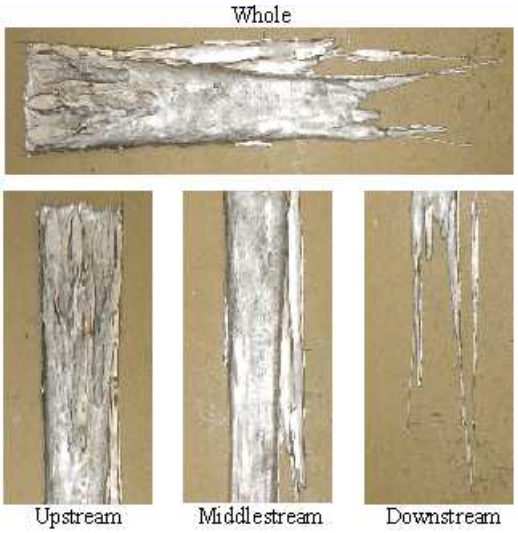

Fig. 2 Photographs of adherence of frozen metal (Coolant: air, Structure: copper).

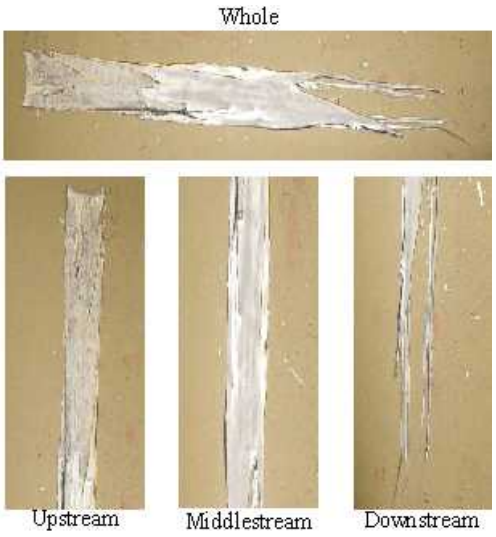

Fig. 3 Photographs of adherence of frozen metal (Coolant: air, structure: stainless steel).

It is clearly seen from the figures that when hot melt falls onto the copper structure, most of the melt is frozen at the upper part of the structure and the frozen layer becomes thick and wide. Whereas, in the case of stainless steel structure, the frozen layer becomes thin and strip. This difference is due to the high thermal conductivity of cooper than stainless steel. This can be explained by the fact that during passing on the copper structure, the molten metal losses significant amount of its sensible latent heat; thus for a very short period of time, the temperature decreased near to its freezing point and become more rapid rate of solidification than the stainless steel structure. Although some instability is found in both the cases at up stream, middle stream and down stream. This instability may be due to the melt initial inertia, buoyancy due to the density difference between the melt, coolant and other hydrodynamic interaction forces.

3.1.2 Water coolant experiment

In case of water coolant experiment, only nozzle no. 1 is used. This is because good adherence of molten metal onto metal structure was found when using nozzle no. 1 during air coolant experiment. This may be due to low mass flow rate (110 g/s) of nozzle no.1 compared to nozzle no. 2 (240 g/s) and nozzle no. 3 (270 g/s).

Figure 4 shows the photographs of experimental results for the water coolant and copper structure that was taken by high-speed video camera. In this case, Wood's metal of 350 g is used as molten metal and the temperature of water coolant was fixed at 50°C. The experiments were performed by changing the melt temperature at the range of 92-120°C. It is seen from these figures that when hot melt falls on the cold copper structure in presence of water coolant, a part of the molten metal is frozen and quenched initially on the structure and a significant amount of molten metal is broken and fall down as different fragments as shown in figures. The fragments include small debris, big debris, sheet like frozen metal etc. Beside these, some frozen metal is broken and fall down due to rapid increase of viscosity. The description of different freezing processes at different positions of **Fig. 4** is given below.

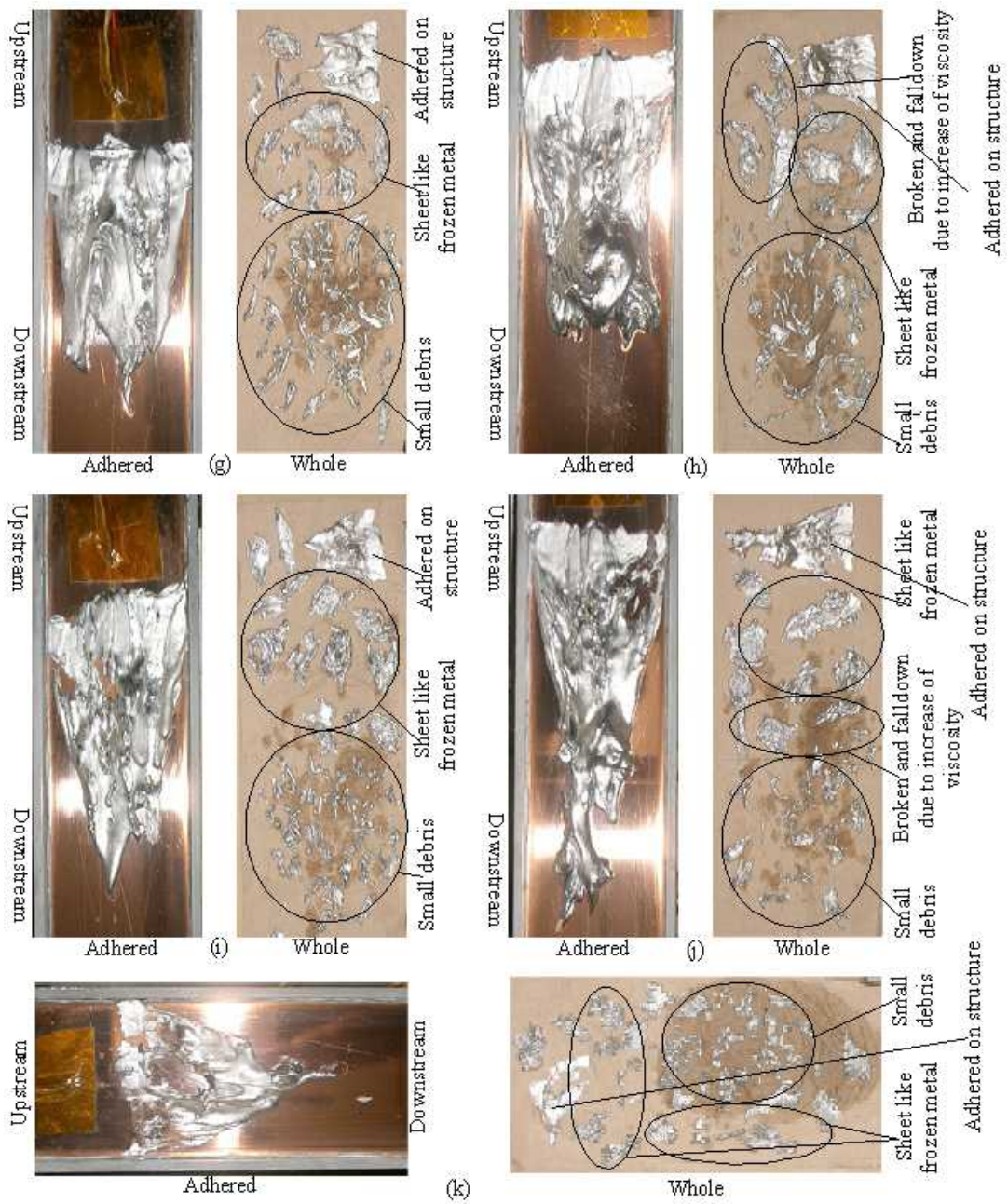

Fig. 4 Photographs of frozen metal (Coolant: water, Structure: copper, Coolant Temp.: 50°C).

Figure 4 (g) shows the photographs at position (g) (melt temperature: 92°C, freezing mode: A_0).

[A_0-1] The melt is poured down in a sheet-like form continuously. When the melt contact with the water, it is quenched forming small size of debris, but slides down continuously without adherence on the structure.

[A_0-2] The melt does not freeze on the structure and debris accumulates at the lower part of the structure.

[A_0-3] The size of the debris becomes large and rolls down on the structure, while frozen metal

appears in a sheet-like form.

[A_0-4] The melt, which rolls down without freezing at this time, starts freezing and adhering on the sheet-like frozen metal, and the frozen metal grows gradually.

[A_0-5] A part of the frozen metal is broken down as debris. As the result, the penetration length does not much change.

[A_0-6] The melt freezes in layers over the frozen metal and then finally stops its flow.

The processes of [A_0-3] and [A_0-4] are main, because they have longest period. The debris formed in the processes [A_0-1], [A_0-2] and [A_0-5], and the sheet-like frozen metal formed in the process [A_0-3] can be seen in the photograph. The cusped shape frozen metal is also observed at the downstream. By increasing the melt temperature, at the point (h), we can observe the different freezing mode from the point (g).

Figure 4 (h) shows the photographs at position (h) (melt temperature: 94-96^{o}C, freezing mode: B_0).

[B_0-1] Similar to the above [A_0-1],

[B_0-2] Similar to the above [A_0-2],

[B_0-3] Similar to the above [A_0-3],

[B_0-4] The melt, which rolls down without freezing till now, freezes at once on the structure with some thickness,

[B_0-5] The melt with enhanced viscosity decelerates and freezes rising continuously above the frozen metal. Then, the melt flows exceeding the penetration length observed in the process [B_0-4] and stops freezing, and

[B_0-6] A part of frozen metal, which is formed as the result of enhanced viscosity, breaks and falls without adherence on the structure because it cannot stand up under its own weight.

The processes of [B_0-4] and [B_0-5] are main, because they have longest period and larger frozen mass. The debris formed in the processes [B_0-1] and [B_0-2], the sheet-like frozen metal formed in the process [B_0-3], and the debris, which broke and fell in the process [B_0-6], can be seen in the photograph. The position where the frozen metal is lifted up in the process [B_0-5] is also observed. Between the melt temperature, 98 and 105°C, we observe a similar freezing mode to A_0.

Figure 4 (i) shows the photographs at position (i) (melt temperature: 98-105^{o}C; freezing mode: A_1). This freezing mode is similar to the mode A_0, but the period for the processes [A_1-1] and [A_2-2] becomes a little bit shorter, and one for the process [A_2-3] becomes a little bit longer.

The amount of small-size debris at the position (i) is less than that at (g), and the amount of sheet-like frozen metal at the position (i) is much than that at (g). There is no piled-up frozen metal due to enhanced viscosity, but the cusped shape frozen metal is observed at the downstream. Between the melt temperature, 106.5 and 108.5 °C, we observe a similar freezing mode to B_0.

Figure 4 (j) shows the photographs at position (j) (melt temperature: 106.5-108.5^{o}C, freezing mode: B_1). There is less break and fall of frozen metal compared with the process [B_0-6] in the mode B_0 and the melt stays on the structure together with the frozen metal. Between the melt temperature, 110 and 120 °C, we observe an almost similar freezing mode to A_0 and A_1.

Figure 4 (k) shows the photographs at position (k) (melt temperature: 110-120^{o}C; freezing mode: A_2). The time period for the processes [A_2-1] and [A_2-1] becomes a little bit shorter, and one for the process [A_2-3] becomes a little bit longer.

The amount of small-size debris at the position (k) is less than that at (i) and (j), and the amount of sheet-like frozen metal at the position (k) is much than that at (i) and (j). There is no lifted-up frozen metal due to enhanced viscosity, but the cusped shape frozen metal is observed as the downstream.

Figure 5 shows the photographs of molten metal for water coolant and stainless steel structure at coolant temperature of 50^{o}C. When hot melt is falling on cold stainless steel structure, it is quenched on structure and small debris, sheet like frozen metal and big debris are found as well as some metal is broken and fall down due to rapid increase of viscosity. In stainless steel structure, instability is found higher than the copper structure. Though the penetration of molten metal on cooper structure is shorter than the stainless steel structure but adherence is more uniform on cooper

structure than the stainless steel structure due to the loss of energy of melt on copper structure is higher than the stainless steel structure. The description of different freezing processes at different positions of **Fig. 5** is given below.

Figure 5 (l) shows the photographs at position (l) (melt temperature: 92-98°C; freezing mode: B_2).

[B_2-1] Similar to the process [B_0-1] in the mode B_0, but smaller amount of debris,

[B_2-2] Similar to the process [B_0-2] in the mode B_0,

[B2-3] A small amount of melt that freezes into debris with large-scale size rolls on the structure,

[B_2-4] The melt, which rolls down without freezing till now, freezes at once and then adheres on the structure with some thickness,

[B_2-5] The melt runs off continuously decelerating on the frozen metal, and falls down forming large-scale debris at the midstream,

[B_2-6] The melt with increased viscosity decelerates gradually, and then freezes rising continuously above the frozen metal, and

[B_2-7] The melt freezes in layers over the frozen metal and then finally stops its flow. The processes of melt break and fall as observed in the mode B_0 does not appear here.

The processes of [B_2-4] and [B_2-5] are main, because they have larger frozen mass. The debris formed in the process [B_2-1], and the large-size debris formed in the processes [B_2-3] and [B_2-5] can be seen in the photograph. The frozen metal similar to the position (j) in the case of copper structure is also observed at the downstream. Although the process [B_2-5] is not observed in the mode B_0, the main processes [B_2-4] and [B_2-5] are similar to those of the mode B_0, there is a similarity to the mode B_1 in the characteristics of the frozen metal on the structure. Therefore, the above processes are called the mode B_2.

Figure 5 (m) shows the photographs at position (m) (melt temperature: 100°C, freezing mode: B_3).

[B_3-1] Similar to the process [A_0-1] in the mode A_0,

[B_3-2] Similar to the process [A_0-2] in the mode A_0,

[B_3-3] Similar to the process [A_0-3] in the mode A_0,

[B_3-4] Similar to the process [A_0-4] in the mode A_0,

[B_3-5] Similar to the process [A_0-5] in the mode A_0, but the size of debris is larger than one observed in the mode A_0, and

[B_3-6] The observed melt behavior is close to the process [B_2-6] in the mode B_2, but the phenomenon such that the melt freezes rising continuously above the frozen metal dose not observed.

The processes of [B_3-4], [B_3-5] and [B_3-6] are main, which combines the features in the main processes of the modes A and B. Therefore, the temperature where this mode appears might be a transient one where the freezing mode changes.

Figure 5 (n) shows the photographs at position (n) (melt temperature: 104°C, freezing mode: B_3). This freezing mode observed here is similar to the mode B_2. The amount of debris formed in the process [B_3-1] is less than in the mode B_2, and the amount of debris formed in the process [B_3-2] is much than in the mode B_2. In the process [B_3-6], the phenomenon such that a part of frozen metal, which cannot adhere on the structure, breaks and falls are observed.

Figure 5 (o) shows the photographs at position (o) (melt temperature: 105-110°C, freezing mode: A_3). This freezing mode observed here is similar to the mode A_2. The amount of debris formed in the process [A_3-2] is much than in the mode A_2, and the amount of the sheet-like frozen metal in the process [A_3-3] is less than in the mode A_2. In the process [A_3-4], the melt rolls down on the sheet-like frozen metal without freezing, and forms large size of debris. Then, the process moves to [A_3-5] and [A_3-6], but the time period for the process [A_3-6] is shorter, and the melt freezes in layers over the frozen metal at once about the same time when the melt finally stops its flow. The penetration length also becomes longer at once during this process.

The processes of [A_3-4] and [A_3-5] are main, and their features such as the frozen metal shape are similar to the mode A_2.

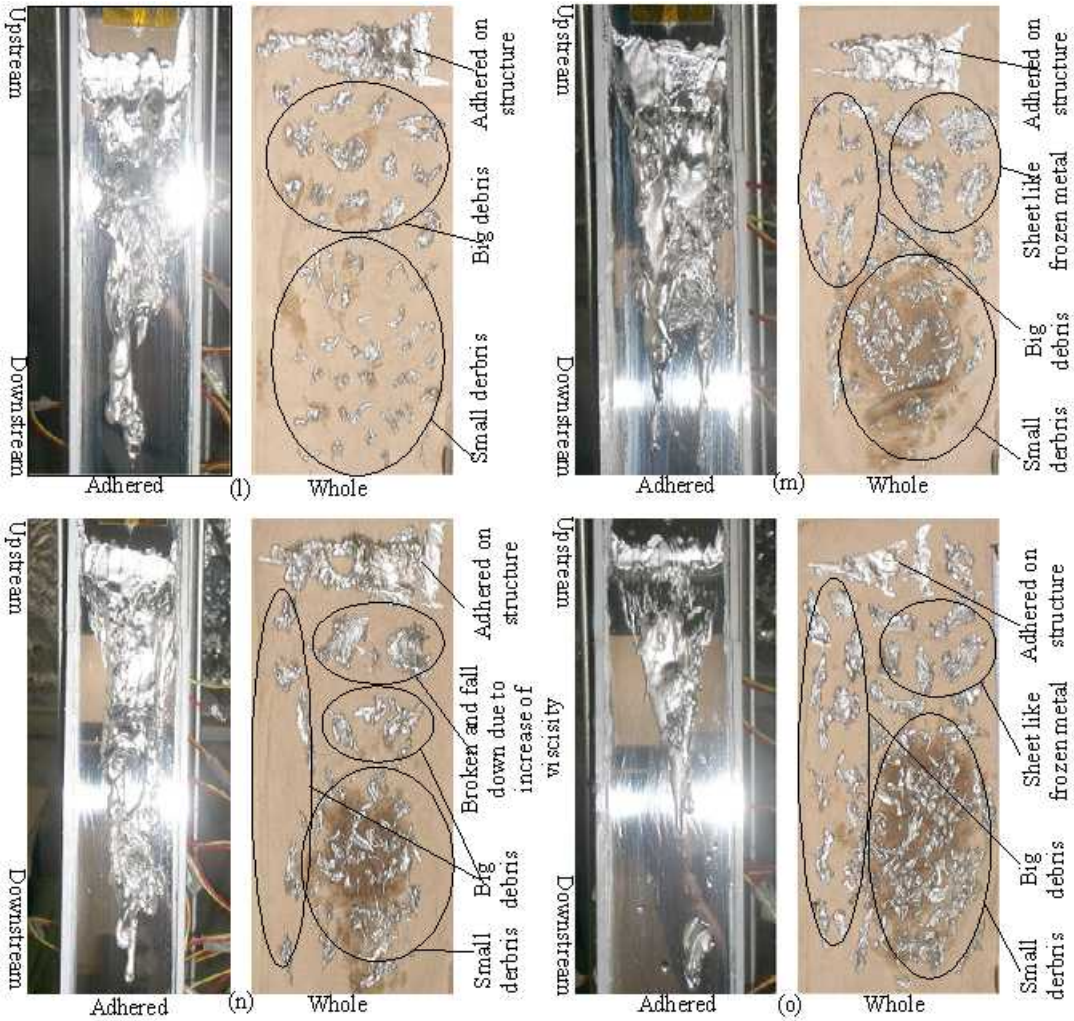

Fig. 5 Photographs of frozen metal (Coolant: water, Structure: stainless steel, Coolant Temp.: 50°C).

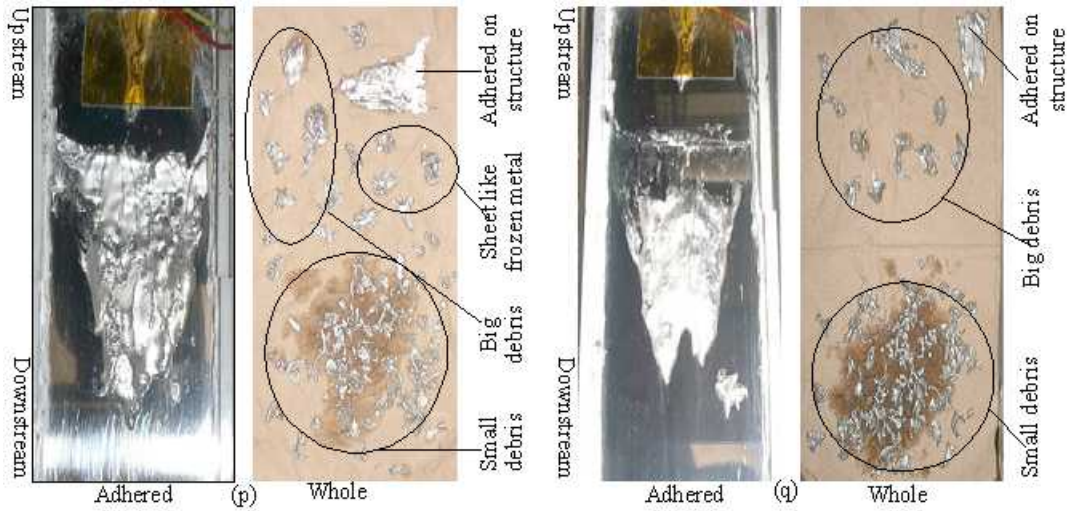

Fig. 6 Photographs of frozen metal (Coolant: water, Structure: stainless steel, Coolant Temp.: 60°C).

Figure 6 shows the photographs of frozen metal for water coolant and stainless steel structure at coolant temperature of 60°C. In this case, Wood's metal of 200g is used as molten metal. When melt falls on stainless steel structure, it becomes quenched and frozen on structure as well as some small debris, big debris and steel like frozen metal is generated. The penetration of adhered frozen metal on stainless steel structure is found shorter during coolant temperature of 60°C than the coolant temperature of 50°C **(Fig. 5)**. These differences may be due to the lower mass of molten metal (200 g) and higher coolant temperature (60°C). The description of different freezing processes at different positions of **Fig. 4** is given below.

Figure 6 (p) shows the photographs at position (p) (melt temperature: 96-100°C, freezing mode: A_4). The freezing mode observed here is similar to the mode A_3. The total amount of the frozen metal is less because the amount of poured melt is 200 g. However, only a little bit sheet-like frozen metal is formed in the process [A_4-3], and the processes [A_4-4] and [A_4-6] is dominant.

Figure 6 (q) shows the photographs at position (q) (melt temperature: 104-130°C, freezing mode: C_0). The freezing mode observed here is different from the mode A_4.

[C_0-1] When the melt lands on the water, it is quenched forming small size of debris, but slides down continuously without adherence on the structure,

[C_0-2] The size of the debris become large and rolls down on the structure, and

[C_0-3] The melt starts freezing and adhering at once as the sheet-like frozen metal on the structure, where less frozen metal exists, and stops its flow almost at the same time.

The period for the processes [C_0-2] and [C_0-2] are very short and the process [C_0-2] is dominant. The debris formed in the process [C_0-2] has the larges portion of the formed debris, compared with the other freezing mode, and this process is main. The freezing behaviors observed in the higher temperature range do not change. As the temperature increases, the melt, which contacts on the water is quenched forming small size of debris, but slides down continuously without adherence on the structure.

Figure 7 shows the photographs of frozen metal for water coolant and stainless steel structure at melt temperature of 92°C. In this case, Wood's metal of 350 g is used as molten metal. This experiment was conducted by changing the coolant temperature where the melt temperature was fixed. When melt falls on stainless steel structure, it becomes quenched and frozen on structure as well as some small debris, big debris and steel like frozen metal is generated. Some metal is also broken and fall down due to rapid increase of viscosity. This experiment was performed for fixing the coolant temperature at maximum penetration and good adherence. The description of different freezing processes at different positions of **Fig. 7** is given below.

Figure 7 (r) shows the photographs at position (r) (melt temperature: 50-53°C, freezing mode: B_4). The frozen metal has a similar shape observed at the position (n) in the mode B_3. The freezing mode observed here is almost similar to the mode B_3.

Figure 7 (s) shows the photographs at position (s) (melt temperature: 54°C, freezing mode: A_5). There is no piled-up frozen metal due to enhanced viscosity, but the cusped shape frozen metal is observed as the downstream.

In addition, there is only a small amount of sheet-like frozen metal and debris, which breaks and falls, are similar to that in the mode A_4.

Figure 7 (t) shows the photographs at position (t) (melt temperature: 56-57°C, freezing mode: B_5). Compared with the mode B_4, the amount of debris formed in the process [B_5-2] is much and the process moves to [B_5-6] in the early stages. The melt behavior such that the frozen metal breaks and falls due to its own weight is observed many times. The melt flow stops without the process [B_5-7]. The main processes [B_5-4] and [B_5-6] are similar to the mode B_4.

The above case suggests that there is no big difference in the freezing behavior between the case, in which the melt temperature is the experimental parameter, and the reverse case, in which the coolant temperature is the experimental parameter. Besides, there is also no big difference in the penetration length between the cases with the copper and stainless steel structures, but the frozen mass tends to increase in the former case. This might be because higher thermal conductivity of copper leads to the melt viscosity enhancement due to the temperature decrease at the upstream, and

melt is easy to freeze in a hump form and to break and fall due to its own weight.

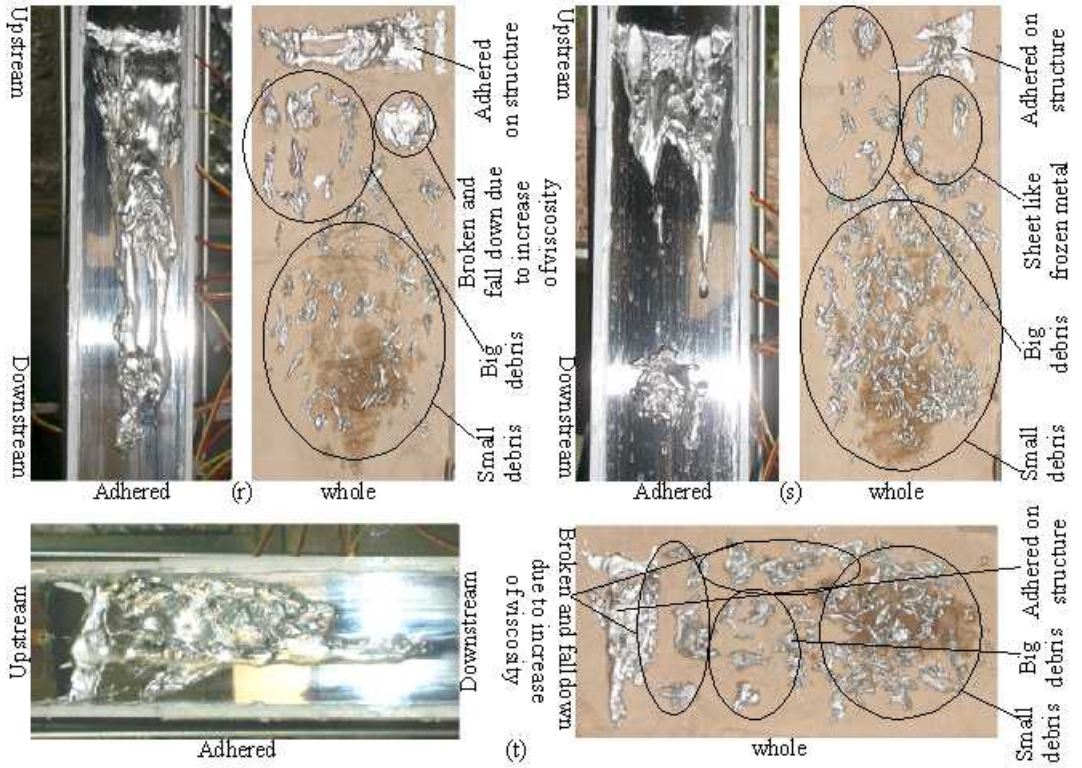

Fig. 7 Photographs of frozen metal (Coolant: water, Structure: stainless steel, Melt Temp.: 92°C).

Considering the various water coolant experiments described above, different freezing modes were developed is illustrated in **Fig. 8**. The freezing modes are defined as mode (A) and mode (B).

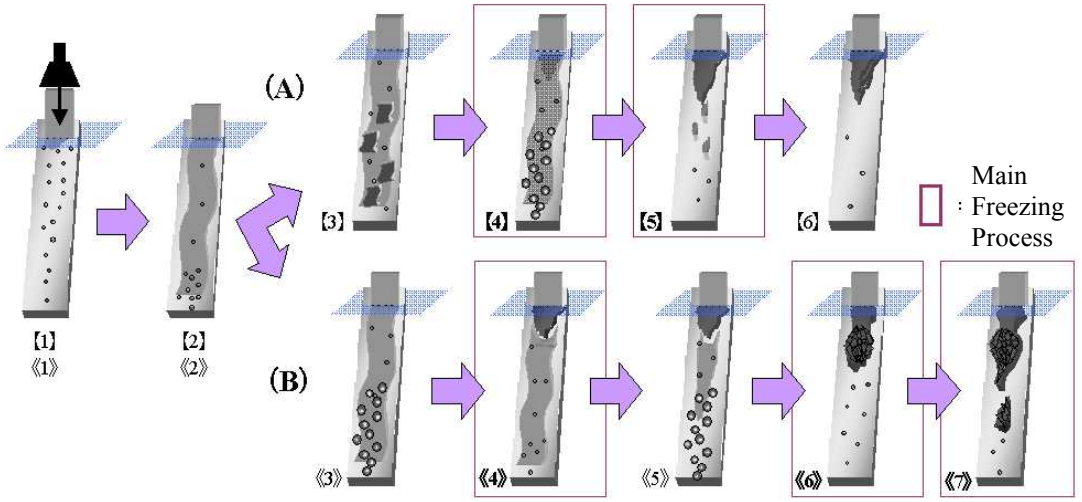

Fig. 8 Freezing mode (A) and (B).

The description of freezing modes (A) and (B) is as follows:

	Freezing mode (A)		Freezing mode (B)
【1】	When melt is falling on structure, it is quenched and generates small debris.	《1》	When melt is falling on structure, it is quenched and generates small debris.
【2】	When melt is continuously falling on structure, some debris is generated at bottom stream.	《2》	When melt is continuously falling on structure, some debris is generated at bottom stream.
【3】	Generate sheet like frozen metal.	《3》	Generate big debris.
【4】	Very thick metal is adhered on structure and big debris is generated.	《4》	Thick metal is adhered and small debris is generated.
【5】	Frozen metal is grown up gradually but a part of metal flow down.	《5》	Thick metal is adhered, some melt flow down and big debris is generated at the middle structure.
【6】	Melt is frozen on the same area of the previous one instantaneously when flow is stopped and penetration length is not changed.	《6》	At rapidly increasing viscosity, frozen metal lifted up.
		《7》	A part of frozen metal is lifted up; some frozen metal is broken and fall down.

3.2 Quantitative analysis

3.2.1 Penetration length and width of air coolant experiment

The penetration length and width of molten metal onto metal structure was measured and plotted as a function of melt temperature and the standard deviation was calculated. **Figure 9** shows the penetration length of copper structure as a function of melt temperature in presence of air coolant. It is found from this figure that the penetration length of frozen metal during passing through the nozzle no. 1 was observed within 28.5-45.9 cm at melt temperature of 100-120°C.

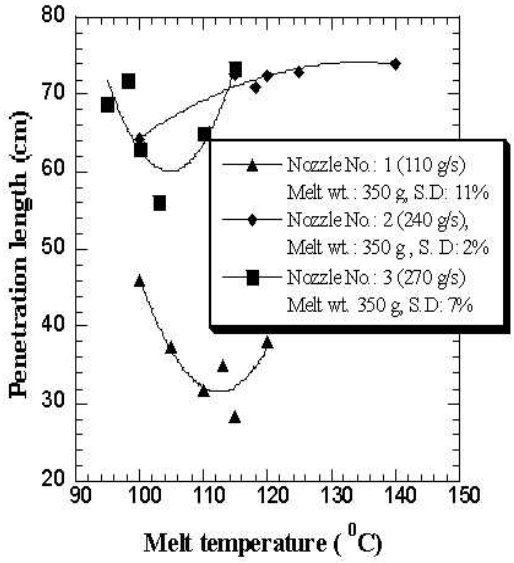

Fig. 9 Penetration length as a function of melt temperature (Coolant: air, Structure: copper).

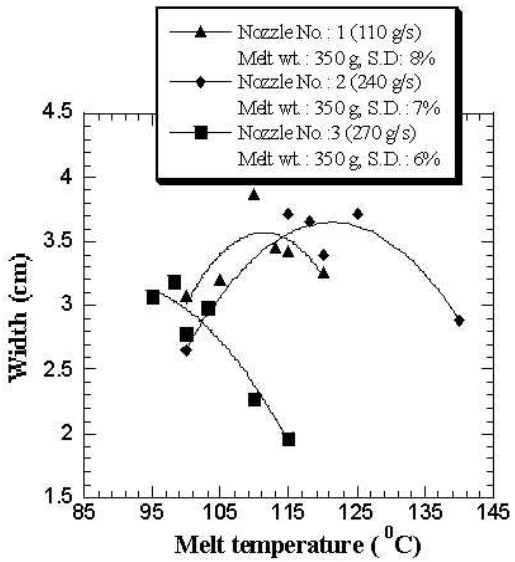

Fig. 10 Width as function of melt temperature (Coolant: air, Structure: copper).

The maximum penetration length was found to be 45.9 cm at melt temperature of 100°C. The penetration length of nozzle no. 2 was found to be within 64.2–74.0 cm at melt temperature of 100–140°C and the maximum penetration length of 74.0 cm was observed at melt temperature of

140°C. The penetration length was found to be 56–73.4 cm using nozzle no. 3 at melt temperature of 98–115°C where maximum penetration length was observed to be 71.8 cm at the melt temperature of 98°C.

Figure 10 shows the width of the frozen metal on copper structure as a function of melt temperature. The width of frozen metal during falling through nozzle no. 1 was found to be in the range of 3.1-3.9 cm at melt temperature of 100-120°C and the maximum width was found to be 3.9 cm at the temperature of 110°C. The width of nozzle no. 2 was found to be in the range of 2.9-3.7 cm at the melt temperature range of 100-140°C where the maximum width of 3.7 cm was observed at melt temperature of 115°C. The width of nozzle no. 3 was measured to be in the range of 2.0-3.5 cm at the range of melt temperature of 95-115°C.

In **Fig. 11**, penetration length of molten metal onto stainless steel structure is plotted as a function of melt temperature. The penetration length of frozen metal when passing through nozzle no. 1 was found to be in the range of 66.5-73.4 cm at melt temperature range of 95-110°C where the maximum penetration length was measured at 73.4 cm at melt temperature of 100.3°C. Using nozzle no. 2, the penetration length was measured in the range of 60.7-71.8 cm at melt temperature range of 95-120°C. The maximum penetration length was found to be 71.8 cm at melt temperature of 108°C.

Figure 12 shows the width of the frozen metal on stainless steel structure as a function of melt temperature. The width of frozen metal during falling through nozzle no. 1 was found to be in the range of 2.2-3.5 cm at melt temperature of 100-120°C and the maximum width was found to be 3.5cm at the temperature of 105°C.The width of nozzle no. 2 was found to be in the range of 2.9-3.7 cm at the melt temperature range of 95-120°C where the maximum width of 3.7 cm was observed at melt temperature of 105°C. The width of nozzle no. 3 was measured to be in the range of 1.9-2.8 cm at the melt temperature range of 90-98°C.

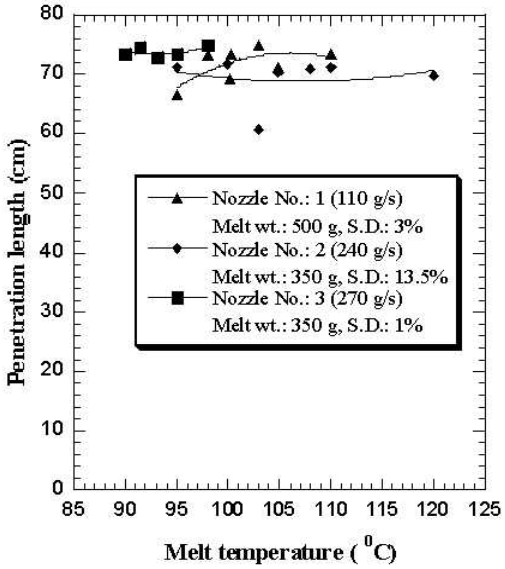

Fig. 11 Penetration length as a function of melt temperature (Coolant: air, Structure: stainless steel).

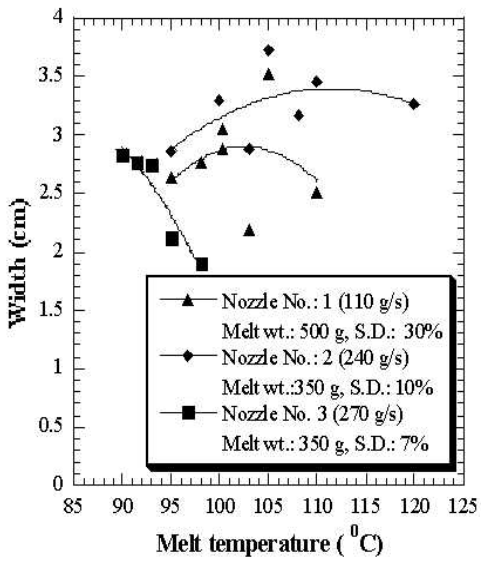

Fig. 12 Width as function of melt temperature (Coolant: air, Structure: stainless steel).

3.2.2 Penetration length and adhered frozen metal of water coolant experiment

Figure 13 shows the penetration length of molten metal on copper structure as a function of melt temperature. It is found from this figure that the penetration length of molten metal on copper structure lies in the range of 7.0–12.5 cm at the temperature range of 92–120°C. The maximum penetration length was found to be 12.5 cm at the melt temperature of 107.5°C. In **Fig. 14**, adhered frozen metal on copper structure are plotted as a function of melt temperature. In case of

adherence of frozen metal on copper structure, the amount of adherence of frozen metal was found to be in the range of 22–91 g at melt temperature range of 92–120°C. The maximum amount of adherence of frozen metal was found to be 91 g at melt temperature of 94°C. A maximum of 27% molten metal was adhered on the copper structure.

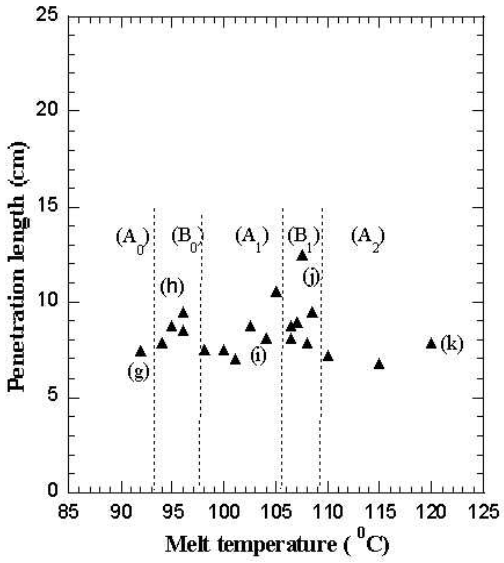

Fig. 13 Penetration length as a function of melt temperature (Coolant: water, Structure: copper, Coolant temp.: 50°C).

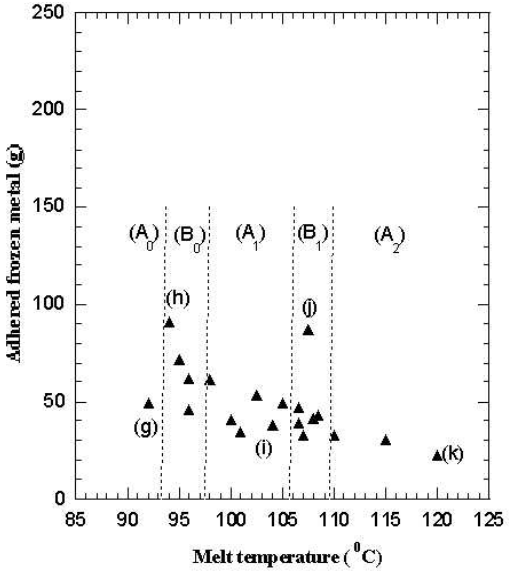

Fig. 14 Adhered frozen metal as a function of melt temperature (Coolant: water, Structure: copper, Coolant temp.: 50°C).

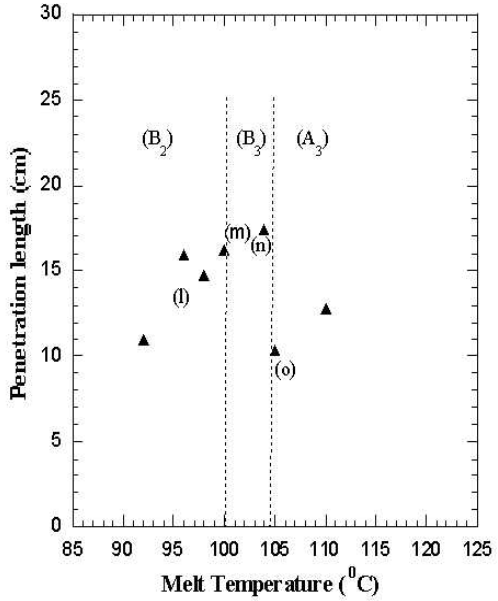

Fig. 15 Penetration length as a function of melt temperature (Coolant: water, Structure: stainless steel, Coolant temp.: 50°C).

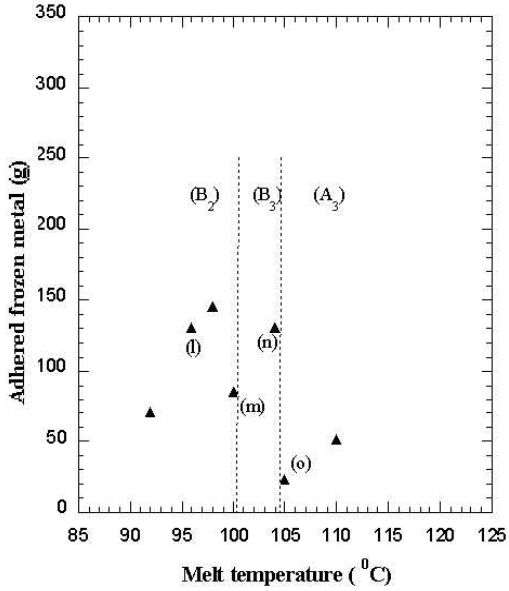

Fig. 16 Adhered frozen metal as a function of melt temperature (Coolant: water, Structure: stainless steel, Coolant temp.: 50°C).

The penetration length of molten metal on stainless steel structure is plotted as a function of melt temperature as shown in **Fig. 15**. It is found from this figure that the penetration length of

molten metal on stainless steel structure lies in the range of 10.3–17.4 cm at the melt temperature range of 96–110°C. The maximum penetration length was found to be 17.4 cm at the melt temperature of 104°C.

Figure 16 shows the amount of adhered frozen metal on stainless steel structure as a function of melt temperature. The amount of adherence of frozen metal on stainless steel structure was found in the range of 24–145 g at the melt temperature range of 96–110°C. The maximum amount of frozen metal was found to be 145 g at the melt temperature of 98°C.In this case, maximum of 23% molten metal was adhered on the stainless steel structure.

The penetration length of molten metal on stainless steel structure for coolant temperature of 60°C is plotted as function of melt temperature as shown in **Fig. 17**. In this case, melt weight of 200 g was used. The penetration length is found to be in the range of 2.5-8.0 cm at the temperature range of 96-130°C. The maximum penetration length was found to be 8.0 cm at melt temperature of 97.5°C. The penetration length for melt temperature of 60°C is found shorter than the penetration length for melt temperature of 50°C **(Fig. 15)** for the same stainless steel structure. This short penetration length may be due to the high melt temperature (60°C) and less mass of melt (200g).

Figure 18 shows the amount of adhered frozen metal on stainless steel structure as a function of melt temperature for coolant temperature of 60°C. The amount of adherence of frozen metal on stainless steel structure was found in the range of 4–45 g at the melt temperature range of 96 –130°C. The maximum amount of frozen metal was found to be 45 g at the melt temperature of 97.5°C. In this case, maximum of 22.5% molten metal was adhered on the stainless steel structure. The maximum penetration length and the maximum amount of frozen metal were found at the same melt temperature of 97.5°C.

Figure 19 shows the penetration length of molten metal on stainless steel structure as a function of water coolant temperature at melt temperature of 92°C. In this case, melt weight of 350 g is used. The penetration length was found in the range of 8.1-17.2 cm water coolant temperature range of 50-58°C. The maximum penetration length was found to be 17.2 cm at water coolant temperature of 52°C.

Figure 20 shows the amount of adhered frozen metal on stainless steel structure as a function of water coolant temperature at melt temperature of 92°C. The amount of adherence of frozen metal was found in the range of 51-126 g at the water coolant temperature range of 50-58°C.

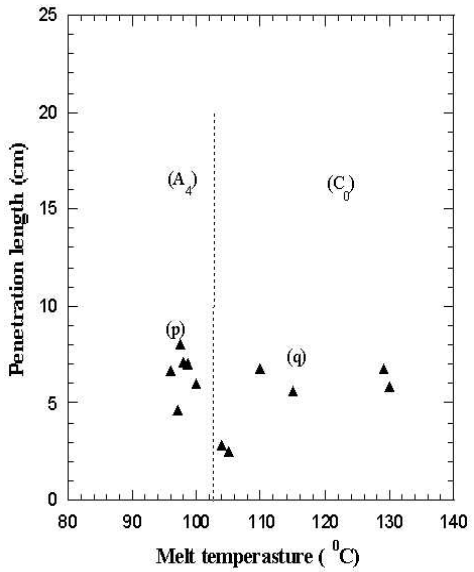

Fig. 17 Penetration length as a function of melt temperature (Coolant: water, Structure: stainless steel, Coolant temp.: 60°C).

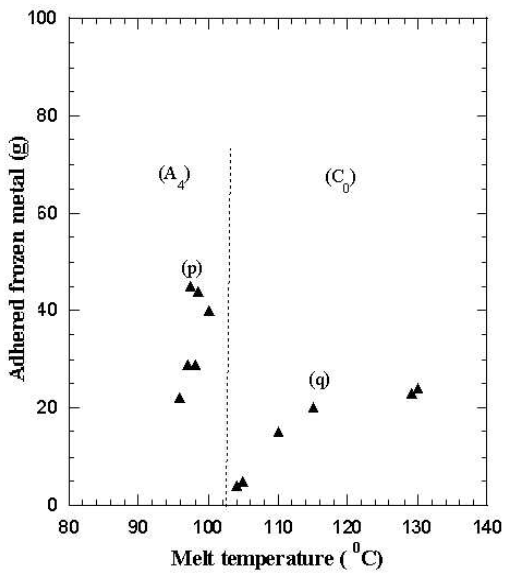

Fig. 18 Adhered frozen metal as a function of melt temperature (Coolant: water, Structure: stainless steel, Coolant temp.: 60°C).

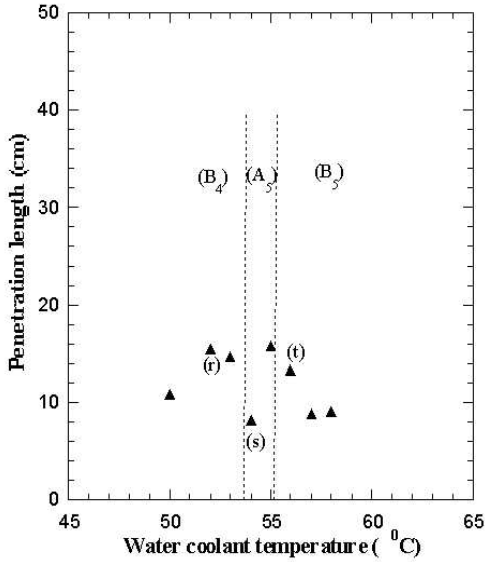

Fig. 19 Penetration length of molten metal as a function of water coolant temperature (Coolant: water, Structure: stainless steel, Melt Temp.: 92°C)

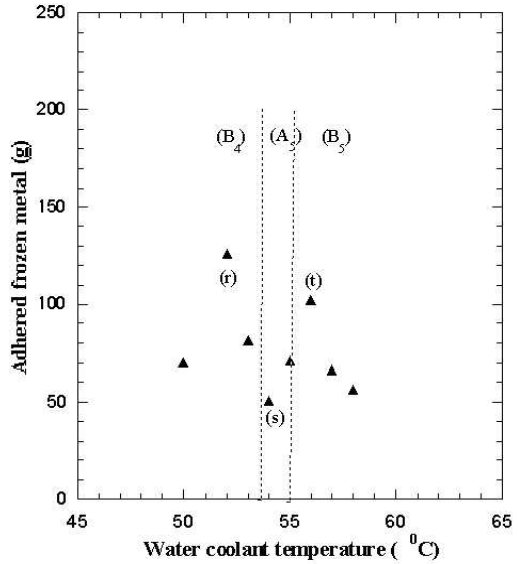

Fig. 20 Adhered frozen metal as a function of water coolant temperature (Coolant: water, Structure: stainless steel, Melt Temp.: 92°C).

The maximum amount of adhered frozen metal was found to be 126 g at the water coolant temperature of 52°C. Though the maximum penetration length and maximum amount of adhered frozen metal was found at the water coolant temperature of 52°C but from the digital video images of different experiments at melt temperature of 92°C, good adherence of molten metal was observed at water coolant temperature of 50°C.

3.3 Comparison between air and water coolant experiments

From visual observation of air coolant experiment described in section 3.1.1, it is clearly observed that the frozen layer becomes thicker and wider on copper structure than that on stainless steel structure. It can also be predicted from the discussion of section 3.2.1 that the penetration length of molten metal on stainless steel structure is little bit higher than on copper structure while on the other hand, the width is found to be a bit higher in copper structure than the stainless steel structure although the penetration of molten metal on copper structure is little bit shorter than that on stainless steel structure which is due to the high thermal conductivity of copper than stainless steel.

From the visual observation of water coolant experiments **(Figs. 4 to 7)**, it is clearly observed that the frozen layer on copper structure is more uniform than that on stainless steel structure and higher instability of frozen layer is also found on stainless steel structure than that on copper structure. The penetration length is found short for both stainless steel and copper structures but it is little bit higher in case of stainless steel structure than that of copper structure. On the other hand, the maximum amount of adhered frozen metal on copper structure is higher (27%) than that on stainless steel structure (23%). This favorable freezing behavior of molten metal on copper structure is due to the loss of energy of melt on copper structure is higher than stainless steel structure.

Comparing the freezing behavior of molten metal between air and water coolant experiments, it is visually observed from the outlook information that in air coolant experiment, most of the frozen metal is adhered on structure and the shape of the frozen metal is found to be thin and wide. The shape of the frozen metal is also found to be uniform with good adherence. Whereas, in water coolant experiment, it is found from the visual observation that only a part of the molten metal is frozen initially on the structure and a significant amount of molten metal is broken and fall

down as different fragments like debris. The debris observed in water coolant experiments is well compared with the debris found by Bang et al.[5] He also used Wood's metal as molten metal of temperature around 90°C and the temperature of water pool was 50°C. The shape of the frozen metal is found to be non-uniform with high instability.

The maximum penetration length of molten metal in air coolant experiment is found to be 74 cm whereas in water coolant experiment it is measured to be 17.4 cm, which is 4.25 times shorter than the air coolant experiment. In air coolant experiment, most of the frozen metal is adhered on structure while in water coolant experiment, maximum of 27% frozen metal is adhered on structure. Beside these, only one freezing mode is found in air coolant experiment where as, different freezing modes are observed in water coolant experiment.

There is no difference in the freezing mode in the cases with air coolant. In the cases with water coolant, the mode converges finally with C type repeating A and B types as the temperature increases. The reason why the A and B modes repeat might be because the structure and coolant temperatures increase near the falling spot of the melt due to the heat exchange caused by the debris formation at the initial stage of the freezing processes.

4. Conclusion

In order to investigate the freezing behavior of molten metal during CDA's for the view point of LMR safety, experiments were performed about the freezing behavior of simulant molten metal. Wood's metal was used as a simulant molten metal. The experiments were conducted using air and water coolant and copper and stainless steel were used as freezing structures. In both the cases, visual information is observed with a high-speed video camera. It is observed from visual information of air coolant experiment that the frozen layer on stainless steel structure becomes more thick and wide than the stainless steel structure. It is also found from this experiment that the penetration length of frozen metal on stainless steel structure is little bit higher than the copper structure but the width is little bit higher in copper structure than the stainless steel structure.

From the visual information of frozen metal in water coolant experiment, it is clearly observed for both the structures that only a part of the molten metal is frozen on the structure and a significant amount of frozen metal is broken and fall down as different fragments. Also high instability is found in stainless steel structure than copper structure due to buoyancy, increasing viscosity and some other interaction mechanisms. In this experiment, short penetration length is found for both copper and stainless steel structure. The maximum amount of adhered of frozen metal was found to be 27% on copper structure and 23% on stainless steel structure.

Comparing the outlook information of freezing behavior of molten metal between the air coolant experiment and the water coolant experiment, it is visually observed that most of the frozen metal is adhered on structure and thin and wide frozen shape of metal with good adherence is found in air coolant experiment where as in water coolant experiment, it is found that most of the frozen metal is broken and fall down as debris as well as a very small fraction is adhered on structure with non uniform shape.

Different freezing modes are observed in water coolant experiment while in air coolant experiment only one freezing mode is observed.

References

1) Sa. Kondo, K. Konishi, M. Isozaki, S. Imahori, A. Furutani and D. J. Brear, Experimental Study on Simulated Molten Jet-Coolant Interactions, Nucl. Eng. Des. Vol. 155, No. 1-2, pp.73-84 (1995).
2) M. Epstein, M. A. Grolmes, Robert E. Henry and Hans K. Fauske, Transient Freezing of a Flowing Ceramic Fuel in a Steel Channel, Nucl. Sci. Eng., Vol. 64, pp.310-323 (1976).
3) R.W. Ostensen, R. E. Henry, J. F. Jackson, G. T. Goldfuss, W. H. Gunther, N. E. Parker, Fuel Flow and Freezing in the Upper Subassembly Structure Following an LMFBR Disassembly,

Trans. Am. Nucl. Soci., Vol.18, pp.214-215 (1974).
4) M. El-genk and A. W. Cronenberg, An Assessment of Fuel Freezing and Drainage Phenomena in a Reactor Shield Plug Following a Core Disruptive Accident, Nucl. Eng. Des. Vol. 47, No. 2, pp. 195-225 (1978).
5) K. H. Bang, J. M. Kim and D. H. Kim, Experimental Study of Melt Jet Breakup in Water, J. Nucl. Sci.Tech., Vol. 40, No. 10, pp. 807-813 (2003).
6) R. N. Smith and E. Meeks, Experimental Investigation of Freezing Inside a Thick-Walled Cylinder, Experimental Thermal and fluid Science, Vol. 7, No. 1, pp. 22-29 (1993).
7) W. Liu, G. X. Wang and E. F. Matthys, Thermal Analysis and Measurements for a Molten Metal Drop Impacting on a Substrate: Cooling, Solidification and Heat Transfer Coefficient, Int. J. Heat Mass Transfer, Vol. 38, No. 8, pp.1387-1395 (1995).
8) W. Peppler, A. Kaiser and H. Will, Freezing of a Thermite Melt Injected into an Annular Channel Experiments and Recalculations, Experimental Thermal and Fluid Sciences, Vol. 1, No. 1, pp. 335-346 (1988).
9) H. K. Fauske, K. Koyama and S. Kubo, Assessment of FBR Core Disruptive Accident (CDA): The role and Application of General Behavior Principles (GBPs), J. Nulc. Sci. Tech., Vol. 39, No. 6, pp. 615-627 (2002).
10) Y. Abe, T. Kizu, T. Arai, H. Nariai, K. Chitose and K. Koyama, Study on Thermal-hydraulic Behavior During Molten Material and Coolant Intraction, Nucl. Eng. Des., Vol. 230, No. 1-3, pp. 277-291 (2004).